Indian Journal of Natural Sciences www.tnsroindia.org.in ©IJONS

Vol.14 / Issue 78 / June / 2023 International Bimonthly (Print) – Open Access ISSN: 0976 – 0997

RESEARCH ARTICLE

Multimodal Brain Tumor Segmentation using 3D-U-Net

Novsheena Rasool[1]* and Javaid Iqbal Bhat[2]

[1]Islamic University of Science and Technology (IUST), Kashmir, India.
[2]Associate Prdofessor, Dept. of Computer Science, Islamic University of Science and Technology (IUST), Kashmir, India.

Received: 11 Apr 2023 Revised: 13 May 2023 Accepted: 31 May 2023

***Address for Correspondence**
Novsheena Rasool
Islamic University of Science & Technology (IUST),
Kashmir, India.
E. Mail: novsheena.rasool@iust.ac.in

ABSTRACT

Brain tumours are the tenth biggest cause of mortality in the world, killing thousands of people each year. Gliomas are the most frequent and severe kind of brain tumour, having a relatively short life expectancy. Thus, treatment planning is essential for improving the quality of life. Magnetic resonance imaging (MRI) is a frequent imaging modality for evaluating these tumours; however, the volume of data generated by MRI prevents manual segmentation in an acceptable amount of time. This demands the employment of automatic segmentation techniques; however, automatic segmentation is difficult due to the great spatial and structural heterogeneity among brain tumours. In this paper, we propose a 3D U-Net deep learning architecture for the semantic segmentation of gliomas. We train our model twice: the first time, we use the bias correction procedure and the minmax scaler normalization in the pre-processing stage, and the second time, we skip the bias field correction technique. Without using bias correction techniques, we found that we still obtained outstanding results. The precision, sensitivity, specificity, dice score, and accuracy metrics are used to evaluate the quality of the segmentation results. We trained and tested our model using the High-Grade Glioma (HGG) of the BRATs 2018 dataset. Our model achieved a maximum Dice score metric of 0.89 for the whole tumour, 0.95 for the core tumour, and 0.90 for the enhancing tumour, with a 98% accuracy rate.

Keywords: Brain Tumor; Segmentation; MRI; Deep Learning; Medical Image Analysis.

INTRODUCTION

Medical imaging is an umbrella term for a variety of non-invasive methods used to view inside the human body without causing any harm. It creates images of internal body organs by using various medical imaging procedures such as MRI, CT scan, ultrasound, and others [18] for diagnostic and treatment purposes and is essential for making proper decisions that will enhance health of millions of people. medical image segmentation plays a crucial role in

processing medical images, Manual segmentation is not effective in removing brain tumours without harming neighboring healthy brain tissue. However Deep Learning in Healthcare [16] particularly, automatic segmentation can be used Automated segmentation can be used to quickly and accurately detect brain tumours[14], which is helpful for making treatment decisions and exact measurements.

Brain tumours are one of the global diseases[17] that must be detected early to save person's life. They are classified as benign and malignant. A benign brain tumour is a collection of cells that grows very slowly in the brain. Malignant brain tumours start in the brain, grow quickly, and aggressively penetrate the surrounding tissues. It can also spread to other parts of the brain and disrupt the central nervous system [14]. Magnetic resonance imaging (MRI) is a popular imaging technique that use radio waves, a computer, and a magnetic field to produce complete, detailed images of organs, soft tissues, bones, and other bodily components [20] and is regarded as one of the best imaging technique for identifying, size, location and shape of brain tumours [19]. It allows medical practitioners to analyze the interior anatomy of the brain and identify specific parts of the brain that are responsible for certain critical activities.T1-weighted MRI,T1-weighted contrast enhancement, T2-weighted, and fluid-attenuated inversion recovery as shown in Fig. 3 are combined to generate a multimodal image with details that can be used for tumour segmentation resulting in significant performance improvement .This is due to the challenge of detecting irregularly shaped tumours using only one MRI modality [15].

Gliomas are the most common type of tumour and are composed of there regions: the core, the enhancing region and the edema. It is difficult to accurately diagnose this form of tumour due to the fact that the cells in different sections of the tumour are not all of the same type[1]. Also, these tumours can form in any section of the brain, and borders between surrounding tissues are fuzzy due to smooth intensity changes, bias field artifacts, and partial volume effects, making tumour volume difficult to determine. Early diagnosis of brain tumours is essential for improving treatment options and survival. However, manual tumour segmentation is a complex, time-consuming, and laborious job due to the large volume of MRI images generated in medical practice [15]. Additionally, soft tissue boundaries of tumours, particularly in gliomas, can make them difficult to distinguish, making it challenging to acquire accurate boundaries tumour regions of the human brain. The remaining portion of this paper is organized as follows: Section 2 highlights previous research, section 3 explains proposed approach, Section 4 provides dataset description and experiment findings, Section 5 provides conclusion and future scope.

RELATED WORK

Dongjin Kwon *et al.* in 2014 [1] proposed a semi-automatic generative technique for multifocal segmentation and registration of glioma brain tumors. Using the brats2013 dataset, dice scores of 0.86, 0.79, and 0.59 were achieved for the complete tumour, core tumour, and enhancing tumour sub region. A semi-automatic Generative system (tumour cut method) for segmenting t1ce brain MRI images was proposed by Andac Hamamci *et al.* in 2012[2] in order to standardize the region of interest and seed selection, the authors used a seeded tumour segmentation approach on t1ce MRI pictures. The proposed technique revealed how the iterative CA architecture or framework, which connects CA (cellular automata)-based segmentation to graph-theoretic techniques, overcomes the shortest path problem. To determine the actual shortest path, authors modify the CA's state transition approach. Additionally, they used a sensitivity variable to address the difficulty of segmenting non-homogeneous tumours, and to impose spatial flatness, they established an inferred level set exterior on a tumour likelihood map derived from CA state data. To begin the procedure, information is obtained from the user simply by drawing a line on the maximum diameter of the tumour. Additionally, a technique based on CA is provided for distinguishing the tissue composition of enhancing and necrotic or core tumours, which is essential for a thorough investigation for response to radiation therapy.

Mostefa *et al.* in 2020[3] introduced a new Deep Convolutional Neural Network architecture to automatically segment glioblastomas (high and low grade) tumours. To improve the quality of the MRI images, smaller portions of lesser than 110 pixels were removed and the CNN model was used to extract more meaningful patterns. The

proposed approach was tested using the BRATS 2018 dataset, which produced results with median dice scores of 0.83 for enhancing tumour sub regions, 0.90 for the whole tumour, and 0.83 for the core tumour. The outcomes of the research showed that the segmentation results were accurate and reliable for classifying different types of tissue in brain MRI images. Mohammad havaei *et al.* in 2016 [4] proposed a novel CNN model to segment glioblastomas autonomously in MR images. The authors employed a two-phase training strategy to address the imbalance in tumour labelling. The proposed method extracts both local and global contextual characteristics simultaneously. The output of an initial Convolutional Neural Network acts as a secondary source of data or information for the subsequent CNN in the proposed cascaded system. Experimental results on brats 2018 dataset showed that the proposed technique achieved dice score outcomes of 0.85 for the whole tumour, 0.78 for the Core tumour, and 0.73 for the enhancing tumour sub region.

R. Pitchai *et al.* in 2021[5] presented an automated brain tumour segmentation system using a combination of the fuzzy K-means approach and an artificial neural network (ANN). The Wiener filter, followed by ANN, was used to reduce noise and classify brain MRI images into healthy and diseased classes. And finally, a fuzzy K-means algorithm was used to locate the tumour from abnormal images. On the BRATS dataset, performance was evaluated using accuracy, sensitivity, and specificity, authors obtained 99% specificity, 94% accuracy, and 98% sensitivity. Dvorak *et al.* in 2015 [6] developed a technique for 3D segmentation of multimodal brain tumour MRIs that relies on local structure prediction utilizing a convolutional neural network model. The provided technique outperformed conventional techniques in predicting voxel-wise labels. The authors tested their approaches using the BRATS2014 dataset, which is openly available, and obtained cutting-edge findings in less than 13 seconds of processing time per volume.

Andriy Myronenko *et al.* in 2015[7] proposed a semantic segmentation network of brain tumours in MRI images using an encoder-decoder architecture to identify tumour subregions from 3-d MRI images. The authors used a vibrational auto-encoder branch to standardize the common decoder and apply extra restrictions to its neural layers. Because of the short training dataset, they employed a vibrational auto-encoder branch to recreate the original input image and increased the number of filters or network width, resulting in consistently better outcomes. The results obtained for enhancing core tumour had an average dice score of 0.7664, the whole tumour had 0.8839 and 0.8154 for core tumor. The proposed technique won first place in the BraTS 2018 competition. GuotaiWang *et al.* in 2017[8]developed a cascaded anisotropic convolutional neural network for automated brain MRI segmentation into three hierarchical regions: whole tumour, core tumour, and enhancing core tumour. In the first phase, the authors segmented the whole tumour; in the second phase, the tumour core was segmented using the result of the first phase's bounding box. To reduce false positives, proposed networks incorporate layers of dilated and anisotropic convolution filters with multi-view fusion and residual connections and multiple-scale predictions to improve segmentation performance. The technique enhanced the enhancing tumour, whole tumour and tumour core, with average Dice values of 0.7859, 0.9050, and 0.8378 on the BraTS 2017 dataset.

METHODOLOGY

Bias Field Correction

Due to the irregularities in the magnetic fields of the MRI machine. The bias field, a low-frequency unwanted signal that affects pixel intensity values and reduces the effectiveness of processing models, has a negative impact on MRI images. It is critical to eliminate bias or variable frequency from MRI images during the pre-processing step in order to increase algorithm performance. We use the N41TK approach [11] to correct the bias in the BRATS2018 dataset. N41TK was created by merging the strong B-spline approximation method with a new optimization approach called nonparametric non uniform normalization (N3).

Normalization

Normalization is the process of converting data such that all characteristics are on an equivalent scale, typically between 0 to 1. It is helpful for training the model since it equalizes all features, which helps to stabilize the gradient descent.

$$X_{scaled} = \frac{X - X_{min}}{X_{max} - X_{min}} \quad (1)$$

3D-UNet Architecture for Segmentation

In this paper, we aim to address the issue of brain tumour segmentation by putting forth a novel network architecture based on U-Net [9]. The UNet deep learning architecture is the most popular architecture for segmenting biomedical images.It is composed of a contracting or down sampling path and expanding or up-sampling path. In the down sampling path, we create a convolution block that captures an increasing number of high-level, abstract features related to the context of the Mri images. Next, we use the Max Pooling operation with a 2 stride to reduce the resolution by two. The convolution block consists of two consecutive 3x3x3 filters, each accompanied by "Selu" nonlinearity and a Lecun Normal kernel initializer. At a certain level, the total number of kernels are constant, but double what it was at the previous level. The up-sampling path employs deconvolution layers to simultaneously learn parameters for transforming a low-resolution image into a high-resolution one, while also retaining enough feature mappings to provide high resolution segmentations with sufficient context information.Furthermore, feature maps from the encoder path are concatenated with feature maps of the decoder path at the same level to keep track of crucial information encoded by the encoder, assisting in precise localization and accurate bounds. In our model, a multi-channel feature map is represented by each blue box. On top of the box, the channel count is shown. At the lower left corner of the box, the x-y size is displayed. Copied feature maps are represented by white boxes and the various operations are shown by the arrows (see Fig. 4).

Training

We first divided the High-Grade Glioma (HGG) MRIs in the ratio of 80:20 (or 80% for training and 20% for testing). Then we combine each mri's three input modalities, such as t2, t1ce, and flair, and we crop the centre 128x128x128 blocks of combined images to reduce unnecessary background areas surrounding the essential volume. We load and process the multimodal MRIs using a customised data generator while maintaining a small batch size to lower the generalisation error and speed up model learning (see Fig 6). The network receives blocks of size 128x128x128x3 as inputs and generates Soft Max of size 128x128x128x4.We trained the network by utilizing the fit function and reduced the cost function in terms of its parameters using the adaptive moment estimator (Adam). Adam typically uses the first and second gradient moments to update and modify the moving average of the existing gradients The learning rate, which regulates how frequently we want to update our weights, is one of our Adam optimizer's parameters. If we choose a high learning rate, our model may not identify the optimum solution, and if we choose a low learning rate, the best results will most likely need too many iterations. As a consequence, we determined that the learning rate should be set at 0. 0001. Furthermore, we set the number of epochs to 250 (see Fig 2) and use the dropout approach to reduce over fitting in our model. As a result, we use the dice coefficient [10,12], which balances the four classes better than the quadratic or cost function cross-entropy function [15], and evaluate the segmentation for each tumoral by using the DSC (Dice Similarity Coefficient).

$$DSC = \frac{2TP}{(TP + FP) + (TP + FN)} \quad (2)$$

where TP, FN, and FP represent true positive, false negative, and false positive measures, respectively.To ascertain the model's actual performance.

DATASET DESCRIPTION

The main focus of the BraTS 2018 Dataset is the segmentation of intrinsically heterogeneous brain tumours, specifically gliomas, using pre-operative 3D-MRI data from several institutions. BraTS 2018 dataset consists of four

distinct types of magnetic resonance imaging (MR) sequences: T1-weighted images (T1), T2 weighted images (T2), post-contrast T1-weighted images (T1ce), and fluid attenuated inversion recovery (FLAIR). Each of them has 240 x 240 x 155 volumes. Labels for tumour segmentation include necrotic (label 1), edema (label 2), background (label 0), and enhancing tumour (label 4). The dataset includes 210 High Grade Glioma (HGG) patient cases and 75 Low Grade Glioma (LGG) patient cases[13]. we exclusively used HGG images. We divided the HGG dataset into two sections, employing 168 images for training and 42 for testing. Performance on the testing set is measured mostly by segmentation accuracy. The accuracy of the segmentation is assessed using the dice score metrics. The workflow diagram of proposed model is shown in Fig.5.

CONCLUSION AND FUTURE SCOPE

Medical image segmentation divides healthcare images into only the necessary regions, and thus allows more accurate anatomical examination. The most often used imaging technology for segmenting brain tumours is MRI, which produces more detailed pictures [17], and the majority of researchers are employing this method when detecting and segmenting brain tumours. In this paper, we first preprocess HGG of BRATS 2018 datasets using N41TK bias field correction [11] and Min Max scaler normalization techniques, and then we create a 3d-unet model for distinguishing brain tumour pixels from healthy pixels or for segmentation purpose. Even without post-processing, our method reliably predicts tumour cells. Furthermore, we observe that our model produces better results without the bias correction procedure. We evaluated our model based on dice score, accuracy, sensitivity, specificity, and precision, and we obtained extremely good results by training and testing on the NVIDIA Tesla V100 32 GB GPU. Using the Bias Field Correction technique in preprocessing, our model produced dice scores of 0.86,0.83,0.78 for the whole, core, and enhancing tumours respectively, additionally, our model achieved 99% specificity, 98% sensitivity, 98% accuracy, and 98% precision. Contrarily, when we exclude the bias correction procedure from our model, we get results that are more accurate, such as dice scores of 0.89 for the whole tumour, 0.95 for the core tumour, and 0.90 for the enhancing tumour. Additionally, without bias correction, the proposed model generated accuracy, sensitivity, specificity, and precision values of 98%,98%, 99%, and 98% respectively. In the future, we'll attempt new things to see if we can further enhance the dice score, including changing the model architecture or using post-processing techniques Table I & II.

REFERENCES

1. Kwon, D., Shinohara, R. T., Akbari, H., & Davatzikos, C. (2014, September). Combining generative models for multifocal glioma segmentation and registration. In International conference on medical image computing and computer-assisted intervention (pp. 763-770). Springer, Cham.
2. Hamamci, A., Kucuk, N., Karaman, K., Engin, K., & Unal, G. (2011). Tumor-cut: segmentation of brain tumors on contrast enhanced MR images for radiosurgery applications. IEEE transactions on medical imaging, 31(3), 790-804.
3. Akil, M., Saouli, R., & Kachouri, R. (2020). Fully automatic brain tumor segmentation with deep learning-based selective attention using overlapping patches and multi-class weighted cross-entropy. Medical image analysis, 63, 101692.
4. Havaei, M., Davy, A., Warde-Farley, D., Biard, A., Courville, A., Bengio, Y., ... & Larochelle, H. (2017). Brain tumor segmentation with deep neural networks. Medical image analysis, 35, 18-31.
5. R. Nicole, "Title of paper with only first word capitalized," J. Name Stand. Abbrev., in press.
6. Dvořák, P., & Menze, B. (2015, October). Local structure prediction with convolutional neural networks for multimodal brain tumor segmentation. In International MICCAI workshop on medical computer vision (pp. 59-71). Springer, Cham.
7. Myronenko, A. (2018, September). 3D MRI brain tumor segmentation using autoencoder regularization. In International MICCAI Brainlesion Workshop (pp. 311-320). Springer, Cham.

8. Wang, G., Li, W., Ourselin, S., & Vercauteren, T. (2017, September). Automatic brain tumor segmentation using cascaded anisotropic convolutional neural networks. In International MICCAI brainlesion workshop (pp. 178-190). Springer, Cham.
9. Ronneberger, O., Fischer, P., & Brox, T. (2015). U-net: Convolutional networks for biomedical image segmentation. In Medical Image Computing and Computer-Assisted Intervention–MICCAI 2015: 18th International Conference, Munich, Germany, October 5-9, 2015, Proceedings, Part III 18 (pp. 234-241). Springer International Publishing.
10. Isensee, F., Kickingereder, P., Wick, W., Bendszus, M., & Maier-Hein, K. H. (2018). Brain tumor segmentation and radiomics survival prediction: Contribution to the brats 2017 challenge. In Brainlesion: Glioma, Multiple Sclerosis, Stroke and Traumatic Brain Injuries: Third International Workshop, BrainLes 2017, Held in Conjunction with MICCAI 2017, Quebec City, QC, Canada, September 14, 2017, Revised Selected Papers 3 (pp. 287-297). Springer International Publishing.
11. 'https://simpleitk.readthedocs.io/en/v1.2.3/Examples/N4BiasFieldCorrection/Documentation.html'
12. Kermi, A., Mahmoudi, I., & Khadir, M. T. (2019). Deep convolutional neural networks using U-Net for automatic brain tumor segmentation in multimodal MRI volumes. In Brainlesion: Glioma, Multiple Sclerosis, Stroke and Traumatic Brain Injuries: 4th International Workshop, BrainLes 2018, Held in Conjunction with MICCAI 2018, Granada, Spain, September 16, 2018, Revised Selected Papers, Part II 4 (pp. 37-48). Springer International Publishing.
13. Saeed, M. U., Ali, G., Bin, W., Almotiri, S. H., AlGhamdi, M. A., Nagra, A. A., ... & Amin, R. U. (2021). RMU-net: a novel residual mobile U-net model for brain tumor segmentation from MR images. Electronics, 10(16),1962.
14. Hossain, T., Shishir, F. S., Ashraf, M., Al Nasim, M. A., & Shah, F. M. (2019, May). Brain tumor detection using convolutional neural network. In *2019 1st international conference on advances in science, engineering and robotics technology (ICASERT)* (pp. 1-6). IEEE.
15. Cherguif, H., Riffi, J., Mahraz, M. A., Yahyaouy, A., & Tairi, H. (2019, December). Brain tumor segmentation based on deep learning. In *2019 International Conference on Intelligent Systems and Advanced Computing Sciences (ISACS)* (pp. 1-8). IEEE.
16. Malik, M., Singh, Y., Garg, P., & Gupta, S. (2020). Deep learning in healthcare system. *International Journal of Grid and Distributed Computing*, *13*(2), 469-468.
17. 'https://www.cancer.net/cancer-types/brain-tumor/diagnosis#:~:text=MRIs%20create%20more%20detailed%20pictures,are%20different%20types%20of%20MRI.'
18. Iniewski, K. (Ed.). (2009). Medical imaging: principles, detectors, and electronics. John Wiley & Sons.
19. Rasool, N., & Bhat, J. I. (2023, March). Glioma Brain Tumor Segmentation using Deep Learning: A Review. In 2023 10th International Conference on Computing for Sustainable Global Development (INDIACom) (pp. 484-489). IEEE.
20. Sajid, S., Hussain, S., & Sarwar, A. (2019). Brain tumor detection and segmentation in MR images using deep learning. Arabian Journal for Science and Engineering, 44(11), 9249-9261.
21. Zhao, X., Wu, Y., Song, G., Li, Z., Zhang, Y., & Fan, Y. (2018). 3D brain tumor segmentation through integrating multiple 2D FCNNs. In Brainlesion: Glioma, Multiple Sclerosis, Stroke and Traumatic Brain Injuries: Third International Workshop, BrainLes 2017, Held in Conjunction with MICCAI 2017, Quebec City, QC, Canada, September 14, 2017, Revised Selected Papers 3 (pp. 191-203). Springer International Publishing.
22. Zhao, B., Ren, Y., Yu, Z., Yu, J., Peng, T., & Zhang, X. Y. (2021). AUCseg: An Automatically Unsupervised Clustering Toolboxfor 3D-Segmentation of High-Grade Gliomasin Multi-Parametric MR Images.Frontiers in Oncology, 11, 679952.

Table I. Comparison on the HGG Brats 2018 dataset

Ref.	Grade	Method	Data set	Dice Similarity Coefficient		
				WT	CT	ET
[9]	HGG	Shallow U-Net	BRATS 2018	0.467	0.703	0.584
[10]	HGG	U-Net(axial)+3D CRF	BRATS 2018	0.811	0.750	0.754
[18]	HGG	3D-unsupervised method	BRATS 2018	0.8209	0.7089	0.7254

[10]	HGG	FCNNs (coronal, sagittal, axial)	BRATS 2018	0.696	0.800	0.730
[10]	HGG	Fusing (FCNNs+3D CRF) +post-process	BRATS 2018	0.873	0.868	0.828
Proposed Method	**HGG**	**3D-UNet**	**BRATS 2018**	**0.876**	**0.962**	**0.918**

Table II. Results of Our Experiments On Brats 2018 Model Using Proposed Method

Results	Dice Loss	Dice-Coefficient	Accuracy	Sensitivity	Specificity	Precision	Dice Similarity Coefficient		
							WT	CT	ET
Training (without bias field correction)	0.0348	0.9652	0.9943	0.9941	0.9982	0.9945	0.960	0.964	0.932
Testing (without bias field correction)	**0.0731**	**0.9269**	**0.9889**	**0.9887**	**0.9964**	**0.9892**	**0.899**	**0.955**	**0.903**
Training (with bias field correction)	:0.0612	0.9362	0.9914	0.9913	0.9972	0.9917	0.893	0.949	0.906
Testing (with bias field correction)	**0.1908**	**0.8103**	**0.9802**	**0.9807**	**0.9937**	**0.9812**	**0.869**	**0.837**	**0.786**

Table III. Proposed Model Parameter

Total Number of Parameters	Number of Trainable Parameters	Number of Non-Trainable Parameters
90,448,356	90,448,356	0

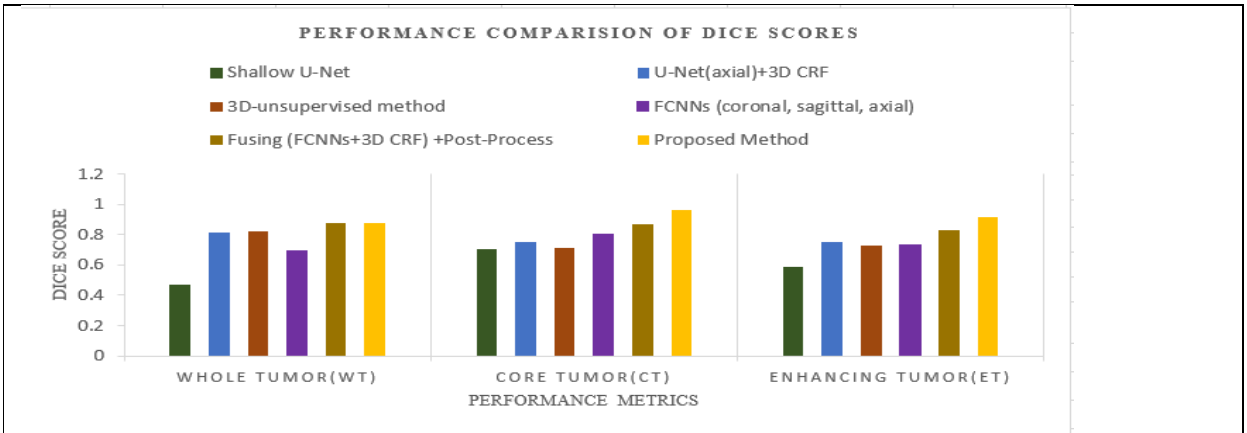

Fig 1. Performance Comparison of Proposed Approach with Other Approaches

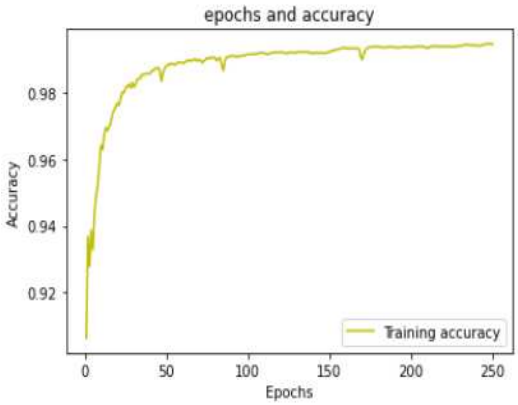

Fig. 2 Training Accuracy Vs Number Of Iterations

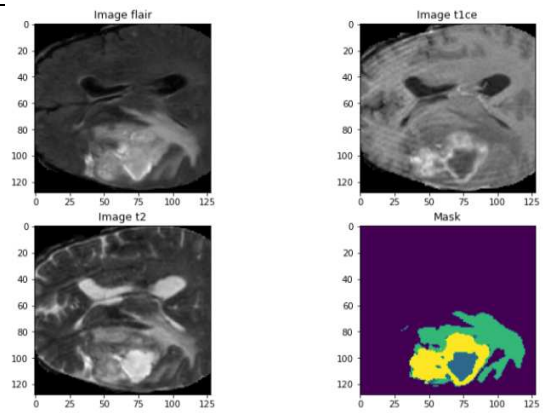

Fig. 3 Input Modalities Flair, T1ce, T2 And Mask

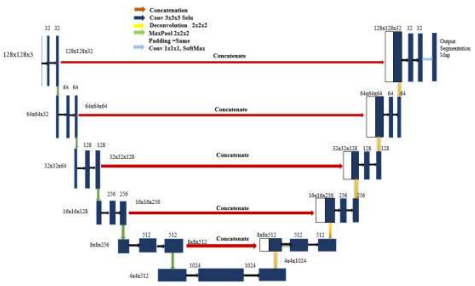

Fig 4. Proposed 3d-U-Net Architecture

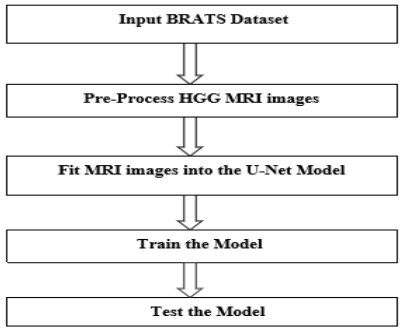

Fig 5. Block Diagram Of Proposed Method

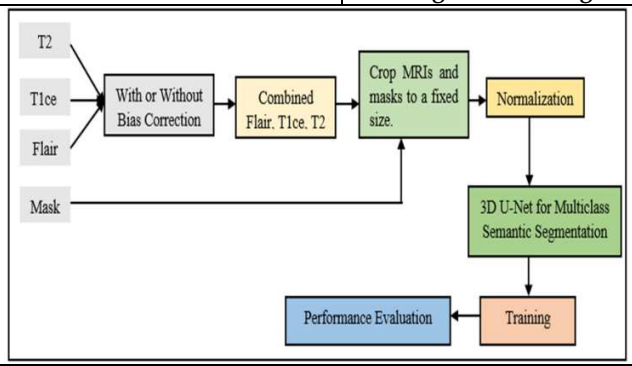

Fig. 6 Block Diagram of Proposed Approach